Tuned Parameters of PID for Optimization of Losses in Magnetic Levitation System

A. Aghazadeh[1], I. Niazazari[1], H. Askarian Abyaneh[1*]

[1]Amirkabir University of Technology, Tehran, Iran

ARTICLE INFO	A B S T R A C T
	In this paper a new method is proposed for determining PID controller parameters in order to decrease losses in levitation system of magnetic trains. It is assumed that this system is a hybrid system and it consists of electric and permanent magnet. For optimization of losses initially AC losses of magnetic levitation system are calculated. Linear model of levitation system as well as modeling the system is offered. The parameters related to PID controller are tuned with Ziegler–Nichols method and optimizing methods using genetic algorithm. The corresponding results are compared.

1. Introduction

Along with the increase in the population and expansion in residential areas, automobiles and air services cannot afford mass transit anymore. Accordingly, demands for innovative means of public transportation have increased. In order to appropriately serve the public, such a new-generation transportation system must meet certain requirements such as rapidity, reliability, and safety. The magnetic levitation (Maglev) train is one of the best candidates to satisfy those requirements. While a conventional train drives forward by using friction between wheels and rails, the Maglev train replaces wheels with electromagnets and levitates on the guideway without any contact [1].

One of levitation technologies that is used in maglev trains is the Electromagnetic suspension (EMS). The levitation accomplished based on the magnetic attraction force between a guideway and electromagnets. This methodology is inherently unstable due to the characteristic of the magnetic circuit. There are two types of EMS levitation technologies. These include: a) the levitation and guidance integrated type; b) the levitation and guidance separated type. EMS types are shown in Figure 1 [1, 2].
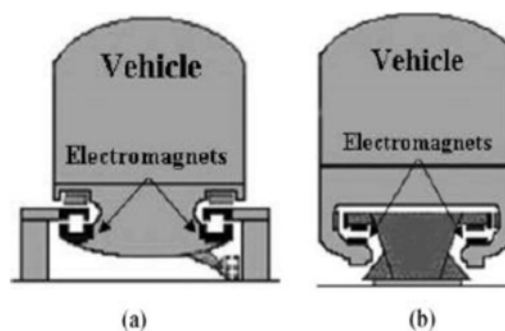

Figure 1. EMS systems: (a) integrated type and (b) separated type [1]

Another technology in levitation system is called the Hybrid Electromagnets (HEMS). In order to reduce the electric power consumption in EMS, permanent magnets are partly used with electromagnets as illustrated in Figure 2. In a certain steady-state air gap, the magnetic field from the PM is able to support the vehicle by itself and the electric power for the

electromagnets that control the air gap can be almost zero. However, HEMS requires a much bigger variation of current amplitude compared with EMS from the electromagnets' point of view because the PM has the same permeability as the air [3].
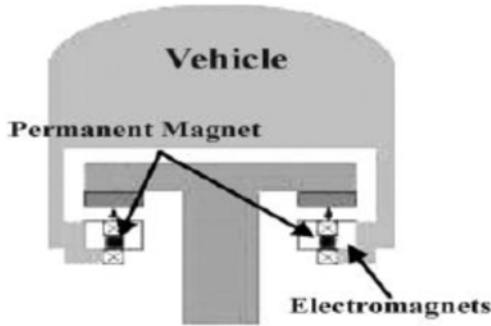

Figure 2. HEMS system [1]

Analysis of the eddy current induced in track on medium-low speed maglev train is reported in [4]. A loss separation method for a high-Speed Magnetic Levitated permanent magnet synchronous motor (PMSM) based on drag system experiment was stated in [5]. Minimization of system-level losses in VSI-based induction motor devices is conveyed in [6]. Techniques for efficiency improvement in PWM motor drives is provided in [7].

In this paper, the linear model of HEMS system is presented. This linear model is achieved by using Taylor series on equilibrium point. Air gap of this system is controlled by PID controller. To tune PID, the Z-N, modified Z-N and genetic Algorithm (GA) methods are used. The air gap and AC losses of each method will be calculated.

2. Hybrid Maglev System

The configuration of a hybrid maglev system is depicted in Figure 3, which consists of a hybrid electromagnet, a ferrous plate and a load carrier. Among these, the hybrid electromagnet is composed of a permanent magnet [2].

Permanent magnets characteristics are usually described by their demagnetization curve. This demagnetization curve, represents the total magnetic flux that is carried in combination by the air and the Permanent

Magnet (PM). This curve is plotted in the second quadrant of a B-H coordinate system where PMs normally operate.
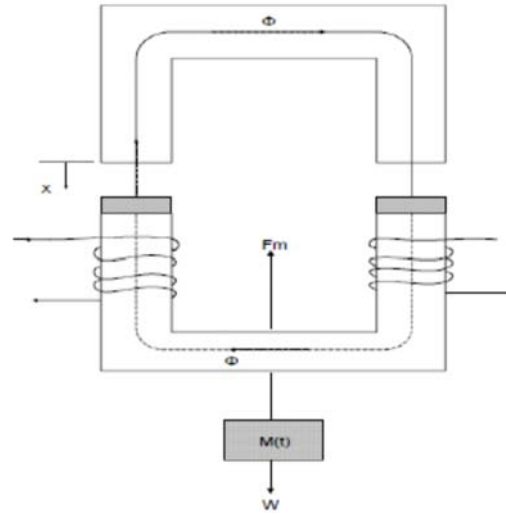

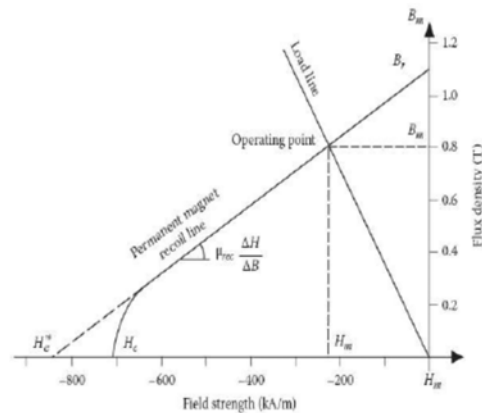
Figure 3. Maglev magnetic circuit [8]

Figure 4. Permanent magnet demagnetization curve [8]

A typical demagnetization curve is shown in Figure 4. The load line, also shown in Figure 4, provides the amount of flux density produced by a PM in a system with a particular geometry and material characteristics, but this production of flux density must be bounded by the PM characteristics and therefore the actual operating point is given by the intersection of the load line and the demagnetization line [8]. The application of Ampere"s Law to the contour shown in Figure 3, provides a means to modeling of PMs. Considering only the PMs in the magnetic circuit of Figure 3, Ampere"s law gives:

$$H_m L_m + H_{ag} L_{ag} = 0 \qquad (1)$$

where H_m and H_{ag} are the magnetic field strength of the PM and air gap, respectively. Also:

$$B_m A_m = B_{ag} A_{ag} = \varphi \qquad (2)$$

where B_m, B_{ag}, A_m and A_{ag} are the flux density in the PM, flux density in the air gap, cross-sectional area of the PM and cross-sectional area of the air gap, respectively [8]. Consideration of the constitutive equation of air $B_{ag} = \mu_0 H_{ag}$ and Equation (2), yields:

$$B_m = -\left(\mu_0 \frac{A_{ag}L_m}{A_m L_{ag}}\right) H_m \qquad (3)$$

where L_{ag} and L_m are the air gap length (also called x) and the thickness of the permanent magnet, respectively. Equation (3) represents the load line of Figure 4. The demagnetization curve can be expressed as:

$$B_m = \mu_r \mu_0 H_m + B_r \qquad (4)$$

where B_r and H_c are the PM retentivity and coercive force, respectively, and $\mu_0 = 4\pi \times 10^{-7}$ H/m is the permeability of free space [8]. Using Equations (3) and (4) to find the intersection between the demagnetization and load lines and supposing $R_m = L_m/(\mu_r A_m)$ and $R_{ag} = L_{ag}/(\mu_r \mu_0 A_{ag})$, gives:

$$B_m = B_r \left(\frac{R_m}{R_{ag}+R_m}\right) \qquad (5)$$

The equivalent magnetic network is shown in Figure 5. The PM is represented by the residual flux generator $\Phi_r = B_r A_m$ in parallel with the reluctance R_m [4].
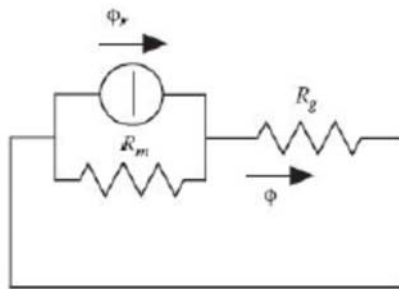

Figure 5. PM equivalent network [8]

The maglev equivalent magnetic circuit is shown in Figure 6. The application of Ampere's Law to this magnetic circuit will provides a means to find λ. Ampere law is written as:

$$2H_m L_m + 2H_{ag} L_{ag} = 2NI \qquad (6)$$

And the load line is:

$$B_m = -\left(\frac{\mu_0 L_m A_{ag}}{L_{ag} A_m}\right) H_m + \left[\frac{\mu_0 A_{ag} N}{A_m L_{ag}}\right] I \qquad (7)$$

Combination of Equations (4) and (7) gives the PM operating point in the presence of coil current.

$$B_m = \frac{NI + H_c L_m}{\frac{x\,A_m}{\mu_0 A_{ag}} + \frac{H_c L_m}{B_r}} \qquad (8)$$

The numerator of this equation shows the contribution of the electromagnet current as well as the permanent magnets to the flux density. This expression is fundamental to finding the attracting magnetic force and the flux linkage λ in the coils. B_m and λ in the coils are related by:

$$\lambda = 2NA_m B_m \qquad (9)$$
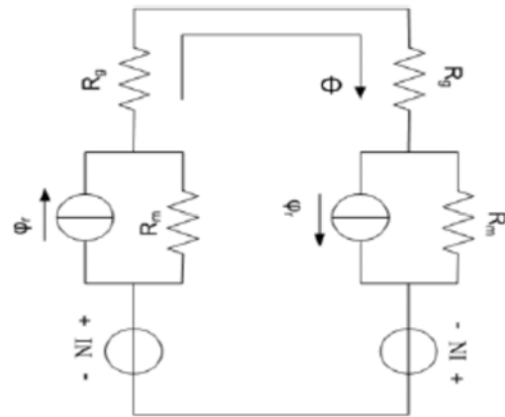
where N is the number of coil turns.

Figure 6. Maglev equivalent magnetic circuit [8]

The magnetic force can be found by considering the magnetic energy stored in the air gap per unit of volume (Energy density). The magnetic force can be found as the energy stored per unit of length. Finally the magnetic force will be:

$$F_m = \mu_0 A_{ag} \left[\frac{N_i + k_1}{x + \mu_0 A_{ag} R_m}\right]^2 \qquad (10)$$

where $K_1 = H_c L_m$.

This expression of the magnetic force will be used in the development of the dynamic model of the maglev system. Equations (8), (9) and (10) can be used to develop an analytical model. A free-model diagram of the maglev mechanical system is depicted in Figure 3. The flux in the electromagnets and permanent magnets produces an attracting force F_m between rotor and stator. This force overcomes the weight of the rotor, to move it upward. Considering the free-body diagram of Figure 3 and Newton's law of motion, Equation (11) describes the dynamic of this mechanical system.

$$m\ddot{X} = mg - F_m \tag{11}$$

where m is the levitated object mass, g is the acceleration of gravity, $\ddot{X}$ is the rotor acceleration and F_m is the magnetic force. Application of Kirchhoff's voltage law and Faraday's induction law to the equivalent electrical circuit of Figure 7, allows derivation of the following equation for the phase voltage.

$$V = ri + \frac{d\lambda}{dx} \tag{12}$$

where r is the coil resistance and λ is the flux linkage in the coil.

$$\Delta V = -\left[\frac{k_2 i_0}{(x_0+N_1)^2} + \frac{(k_2 i_0 + k_3)(N_1 - x_0)}{(x_0+N_1)^3}\right] p \Delta x + \left[r + p k_2 \left[\frac{1}{x_0+N_1} - \frac{x_0}{(x_0+N_1)^2}\right]\right] \Delta i \tag{18}$$

$$\Delta F_M = 2N_2 \left[\frac{N}{x_0+N_1}\right] \left[\frac{Ni_0+k_1}{x_0+N_1}\right] \Delta i - 2N_2 \left[\frac{1}{(x_0+N_1)^2}\right] \left[\frac{Ni_0+k_1}{x_0+N_1}\right] \Delta x \tag{19}$$
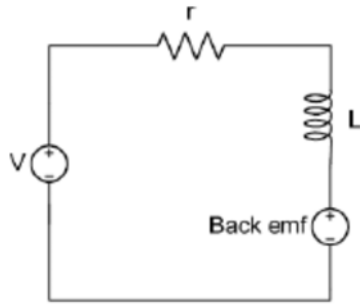

Figure 7. Maglev equivalent electrical circuit [8]

The combination of Equations (8) and (9) yields the following expression of the flux linkage in the coils.

$$\lambda = 2\mu_0 N A_g \left[\frac{N_i + H_c L_m}{x + \mu_0 A_g R_m}\right] \tag{13}$$

where A_g is the air gap cross-sectional area and $R_m = L_m/(\mu_r \mu_0 A_m)$ is the permanent magnet reluctance. The combination of Equations (8), (12) and (13) finally gives the expression used for dynamic modeling of the electromagnetic [2, 8].

$$V = ri + \frac{k_2}{x + A_{ag}R_m\mu_0}\frac{di}{dt} - \frac{dx}{dt}\left[\frac{k_2 i + k_3}{(x + A_{ag}R_m\mu_0)^2}\right] \tag{14}$$

where $K_2 = 2N^2\mu_0 A$, and $K_3 = 2N\mu_0 A K_1$.

3. Linearization by using Taylor Series

For linearization, Taylor's expansion around an operating point can be used. That is, any system variable f_i can be written in terms of a Taylor expansion around its fixed value, f_{io}, as:

$$g(f_i) = g(f_{io}) + g'(f_{io})\Delta f_i + (1/2!)\,g''(f_{io})\Delta f_i{}^2 + \dots \tag{15}$$

where;

$$f_i = f_{io} + \Delta f_i \tag{16}$$

For a function of two variables the same argument can be applied:

$$g(f_1 + f_2) \approx g(f_{10} + f_{20}) + \frac{\partial}{\partial f_1}g(f_{10} + f_{20})\Delta f_1 + \frac{\partial}{\partial f_2}g(f_{10} + f_{20})\Delta f_2 \tag{17}$$

where $\Delta g(f_1, f_2)$ is the last two terms of Equation (17) [9]. If Equations (10) and (14) are expanded by using Taylor series, this yields Equations (18) and (19). These are then the linear equations of electromagnetic force and voltage.

where x_0 and i_0 are the operating points, p=d/dt, $N_1 = A_{ag}R_m\mu_0$ and $N_2 = A_{ag}\mu_0$. The proposed linear model of levitation system that is obtained by using Equations (11), (18) and (19) is shown in Figure 8.

4. PID Controller

PID control is a linear control methodology with a very simple control structure. This type of controller operates directly on the error signal, which is the difference between the desired output and the actual output and generates the actuation signal that drives the plant. KI is integration gain. When KI is small, the system is slow and vice versa. In the design of PID controller the amount of KI is identified to reach to an intended error in steady state. KD is derivation constant. The derivation term acts like predictor, because the speed of change of the error signal affects the control signal. The derivation term has a large effect in systems where disturbances are present, because disturbances are often fast. In PID controller design, KP, KI and KD, related to the closed loop feedback system within the least time is determined and requires a long range of trial and error, (Figure 9) [10].
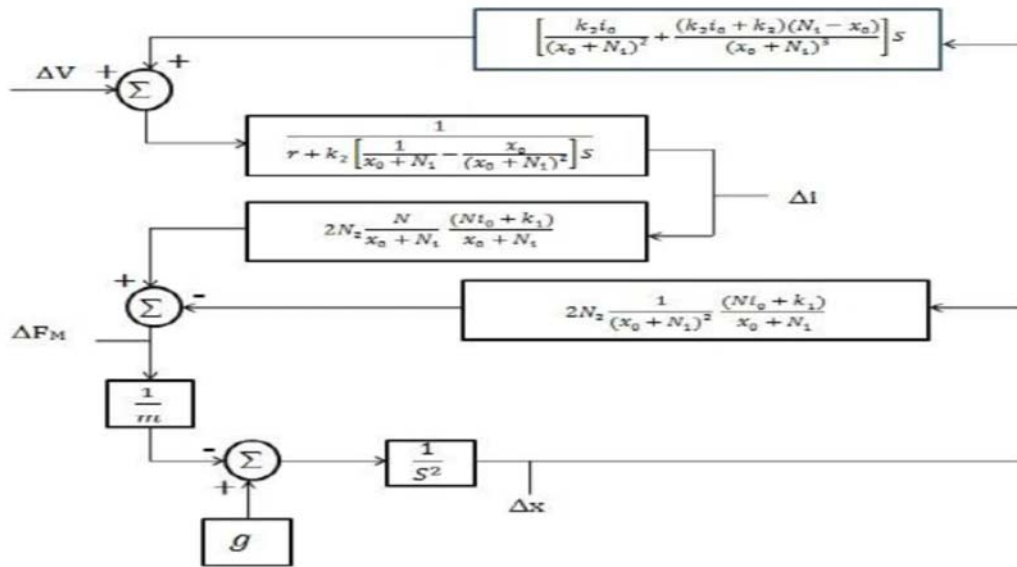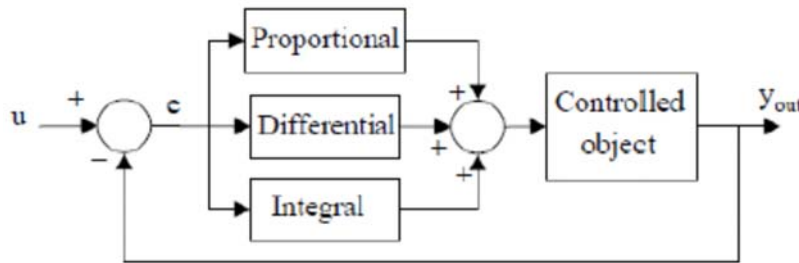
Figure 8. Linear model of levitation system

Figure 9. Close loop PID controlling system [10]

To design a particular control loop, the values of the three parameters (KP, KI and KD) have to be adjusted so that the control input provides acceptable performance from the plant. To get an acceptable solution, there are several controller design methods that can be applied. Two classic methods for tuning the PID parameters are introduced with Ziegler-Nichols in 1942. One of them is celled the frequency response. This method uses a table, critical gain KU and critical period TU to tune PID parameters. KU and TU are determined by using Equation (20) [11].

$$K_u.G(\omega_u)= -1 \qquad T_u=2\pi/\omega_u \qquad (20)$$

ω_n is a frequency that the outcome of Equation (20) in this frequency is equal to -1. After specifying the critical values, by using Table 1 the parameters of PID are tuned. In this table, $T_i=K_P/K_I$ and $T_d=K_D/K_P$.

In Z-N method, damping coefficient is fixed at 0.2155. If designing for the PID parameters needs larger damping coefficient, another method that is the so called Modified Ziegler-Nichols can be used. PID parameters for this method are shown in Equation (21) [11].

Table 1. The Ziegler-Nichols rules (frequency response method) [11]

N	Controller	K_P	T_i	T_d
1	P	$0.5K_u$		
2	PI	$0.45K_u$	$T_u/1.2$	
3	PID	$0.6K_u$	$T_u/2$	$T_u/8$

$$PID:\begin{cases} K = K_u r_b \cos\phi_b \\ T_i = \frac{T_u}{\pi}\frac{(1+\sin\phi_b)}{\cos\phi_b} \\ T_d = \frac{\alpha T_u}{\pi}\left(1 + \frac{\sin\phi_b}{\cos\phi_b}\right) \end{cases} \quad (21)$$

where α = 0.25. For damping coefficients larger than 0.2155, r_b and ϕ_b are shown in Table 2.

Table 2. Coefficients for the modified Z-N [11].

1	ξ	r_b	ϕ_b
2	0.6	0.41	61
3	0.45	0.29	46

5. Genetic Algorithm

Genetic Algorithm (GA) is a stochastic optimization algorithm that mimics the process of natural evolution. The initial information of the Genetic Algorithm to start the calculation is far away from the near correct solution or is simply arbitrary. Therefore, achieving the best solution depends completely to the environment and evolution operators (i.e. selection, crossover and mutation). The algorithm begins the calculation from several independent nods and searches the space which prevents the algorithm from local minimal and suboptimal convergence [12, 13].

Basically, genetic algorithm consists of three main operators including the selection, crossover and mutation.

- Selection
  Selection is a process which selects some fine individuals from the current population to generate matting pool.
- Crossover
  Crossover is composing a pair with every two individuals of the population and exchange parts of Crossover is composing a pair with every two individuals of the population and exchange parts of generated and integrated into the population.
- Mutation
  Altering one or several gene values for each individual of the population is called mutation.

In this research the genetic algorithm is applied to a system to tune the parameters of PID controller and improve controller performance to ensure optimal control performance at the nominal operation condition.

The steps involved in creating and implementing a genetic algorithm are as follows [14]:

- Generate an initial, random population of individual (Chromosomes) for fix size (according to congenital methods KP, KI, KD ranges declared).
- Evaluate the value of the fitness function.
- Select the fitness members of the populations.
- Go to the crossover and mutation operation and make up the new cluster.
- Return to step 2 until reaching at the best value.
- Select the chromosome with the highest fitness as optimal PID controller parameter.

For the purposes of this research it is assumed that IATE is the fitness functions. IATE function is describe in Equation (22).

$$IATE = \int_0^T t|e(t)|\,dt \quad (22)$$

The performance IATE is applied to estimate the PID parameters using PID control tune by GA algorithms and the results are compared with Z-N and modified Z-N methods.

6. Ac Losses

Core loss in a magnetic material occurs when the material is subjected to a time varying magnetic flux. The actual physical nature of this loss is still not completely understood and a simplistic explanation of this complex mechanism is as follows. Energy is used to effect "magnetic domain wall motion" as the domains grow and rotate under the influence of an externally applied magnetic field. When the external field is reduced or reversed from a given value, domain wall motion again occurs to realize the necessary alignment of domains with the new value of the magnetic field. The energy associated with domain wall motion is irreversible and the association with the domain wall motion is irreversible. The energy at which the external field is changed has a strong

Table 3. Parameters of the model

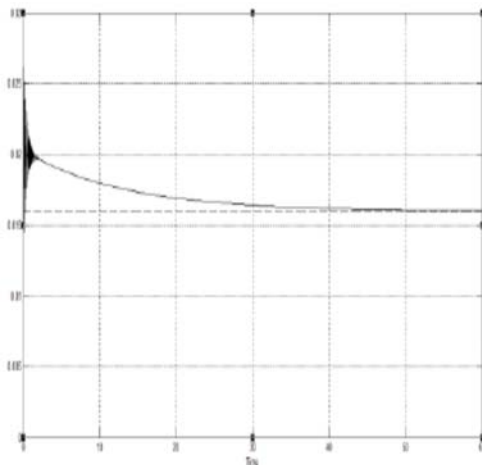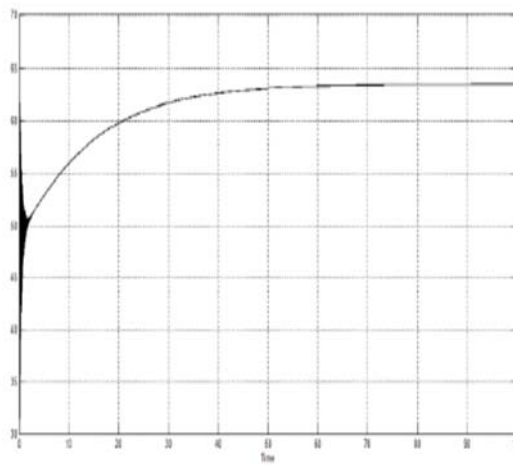| 1	N	400	5	K_1	8380	9	N_2	3.014e-9
2	r	0.75	6	K_2	9.64e-6	10	x_0	0.01
3	g	9.81	7	K_3	0.02	11	i_0	10
4	m	50	8	N_1	0.01	12	X_{ref}	0.016

Figure 10 (a). Air gap

Figure 10 (b): AC losses

influence upon the magnitude of the loss. The loss is generally proportional to some function of the frequency of variation of the magnetic field. The metallurgical structure of the magnetic material, including its electrical conductivity, also has a profound effect upon the magnitude of the loss. In electrical machines, this loss is generally called the core loss [14]. Traditionally, core loss P_c has been divided up into two components: the hysteresis loss P_h and the eddy current loss P_e.

$$P_c = P_e + P_h = k_e\, f^2\, B^2 + k_h\, f\, B^n \qquad (23)$$

where f is the frequency of the external magnetic field, B is the flux density, k_h, k_e and n are the coefficients, which depend on the lamination material, thickness, conductivity, as well as other factors [14]. According to Equation (23), the AC losses in the core are related to B. As a result B reduction can reduce AC losses.

7. Results and Discussion

This research used the linear model that is shown in Figure 8. The parameters of the model are presented in Table 3. The parameters of PID controller are tuned with Z-N, modified Z-N, and the genetic algorithm. The parameters of GA are shown in Table 3. The result of the simulation is depicted in Figures 10, 11 and 12.

Figure 10 shows the results of Z-N tuning method. Figure 10(a) is the air-gap and Figure 10(b) is the curve of AC losses. The resultant value of AC losses is 63.5w.

In Figure 11, the results of modified Z-N are shown. In this method the AC losses is 63.51w that is equal to AC losses in Z-N method.

In Figure 12, the results of the GA in which Equation (26) is the fitness function are presented. In this method the AC losses is 63.4w

8. Conclusions

This study has successfully implemented the PID for the levitated positioning of a hybrid
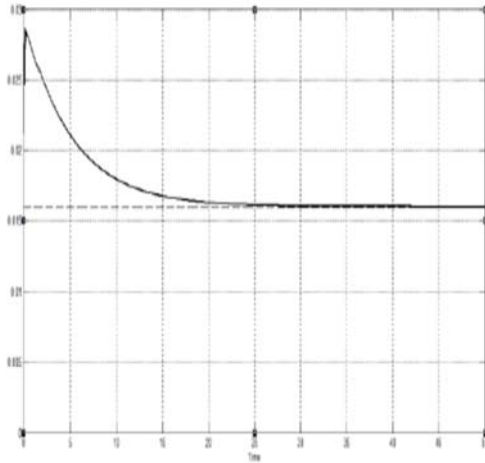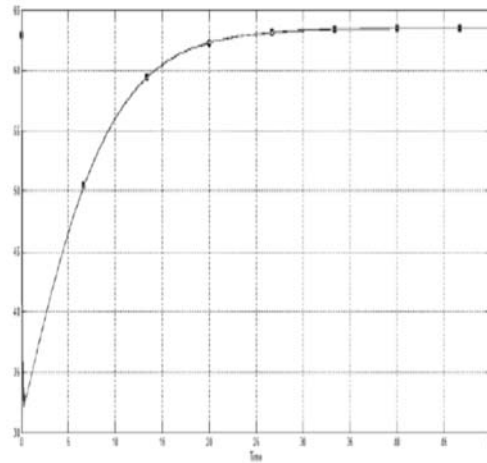
Figure 11 (a). Air gap
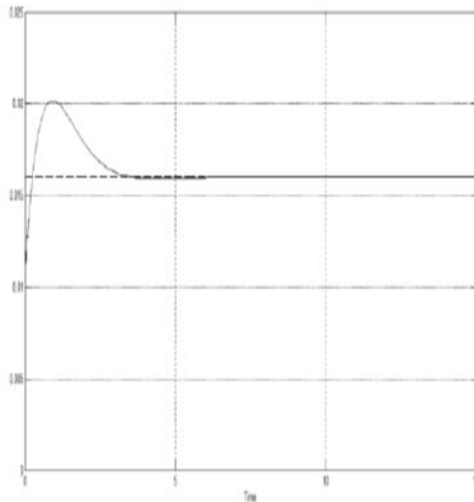

Figure 11 (b). AC losses
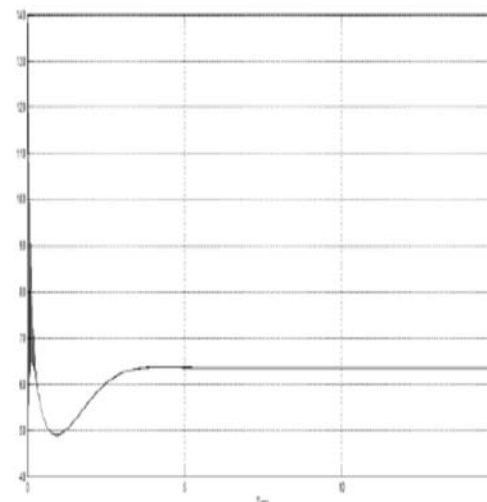

Figure 12 (a). Air gap

Figure 12 (b). AC losses

maglev system to demonstrate their individual control diversities. Performance comparisons of the PID that tune with three different kind of tuning methods are summarized. The speed of the Z-N is too slow and settling time of Z-N is more than 50s. Speed of the modified Z-N is better than Z-N but still is not good. Settling time of modified Z-N is around 30s. On the other hand, the speed of the system which was tuned with GA is faster than Z-N and modified Z-N. Settling time of GA is around 5s. The value of AC losses in system that was tuned by GA is much better than the other methods.

References

[1] H. Lee, K. Kim, J. Lee, Review of Maglev Train Technologies, *IEEE Trans. Magn.,* Vol. 42, No. 7, (2006), pp.1917-1925.

[2] R.J. Wai, J.D. Lee, Performance comparisons of model-free control strategies for hybrid magnetic levitation system, *IEE Proc. Electr. Power Appl.,* Vol. 152, No. 6, (2005), pp. 1556-1564.

[3] Technical survey of the maglev train, (2004), Korea Railroad Research Institute, pp. 150–151.

[4] Guanchun Li, Zhen Jia, Guang He and Jie Li, Analysis of eddy current induced in track on medium-low speed maglev train, IOP

Conference Series: Earth and Environmental Science, Vol. 69, (2017), Conference 1.

[5] Xu Liu, Gang Liu, Bangcheng Han, A loss separation method of a high-speed magnetic levitated PMSM based on drag system Experiment without Torque meter, IEEE Transactions on Industrial Electronics, Vol.66, Issue 4, (2018), pp. 2976-2986.

[6] S. Sridharan, P.T. Krein, Minimization of system-level losses in VSI-based induction motor drives: Offline strategies, *IEEE Trans. Ind. Appl.*, Vol. 53, No. 2, (2017), pp. 1096-1105.

[7] M. Carmela, D. Piazza, M. Pucci, Techniques for efficiency improvement in PWM motor drives, *Electr. Power Syst. Res.*, Vol. 136, (2016), pp. 270-280.

[8] E.R. Noboa, Position sensorless control of a magnetically levitated (MAGLEV) system, The University of Texas at Arlington, August 2010.

[9] R.C. Dorf, R.H. Bishop, Modern Control System, Ninth Edition.

[10] A. Jalilvand, A. Kimiyaghalam, A. Ashouri, H. Kord, Optimal tuning of PID controller parameters on a DC motor based on advanced parameters swarm optimization algorithm, International Journal on Technical and Physical Problems of Engineering (IJTPE) Journal., Vol. 3, No. 4, (2011), pp. 10-17.

[11] C.C. Hang, K.J. Astrom, W.K. Ho, Refinements of the Ziegler-Nichols tuning formula, IEE Control Theory and Application, Vol. 138, No. 2, (1991), pp. 111-118.

[12] M. Seyedkazaemi, A. Akbarimajd, A. Rahnamaei, A. Baghbanpourasl, A genetically tuned optimal PID controller, Proceedings of the 6th WSEAS Int. Conf. on Artificial Intelligence, Knowledge Engineering and Data Bases, Corfu Island, Greece, February 16-19, 2007.

[13] A.H. Fathi, H. Khaloozadeh, M.A. Nekoui, R. Shisheie, Using PSO and GA for optimization of PID parameters, International Journal of Intelligent Information Processing (IJIIP) Vol. 3, No. 1, March 2012.

[14] Y. Chen, P. Pillay, An improved formula for lamination core loss calculations in machines operating with high frequency and high flux density excitation, Conference Record of the 2002 IEEE Industry Applications Conference. DOI:10.1109/IAS.2002.1042645.